Turkish Journal of Electrical Engineering & Computer Sciences

http://journals.tubitak.gov.tr/elektrik/

Research Article

Turk J Elec Eng & Comp Sci
(2014) 22: 43 – 56

doi:10.3906/elk-1206-45

Modeling and simulation of deadbeat-based PI controller in a single-phase H-bridge inverter for stand-alone applications

Tow Leong TIANG*, Dahaman ISHAK
School of Electrical and Electronic Engineering, Engineering Campus, Universiti Sains Malaysia, Nibong Tebal, Penang, Malaysia

Received: 11.06.2012 • **Accepted:** 17.09.2012 • **Published Online:** 20.12.2013 • **Printed:** 20.01.2014

Abstract: This paper presents a deadbeat-based proportional-integral (PI) controller for a stand-alone single-phase voltage source inverter using a battery cell as the primary energy source. The inverter system is simulated in MATLAB/Simulink. It consists of a lead acid battery, third-order Butterworth low-pass DC filter and AC filter, H-bridge inverter, step-up transformer, and a variety of loads, as well as its sinusoidal pulse-width modulation (SPWM) deadbeat-based PI controller. In this paper, 2 simulation case studies are carried out, which are the abrupt load changes from a 400 W resistive load to a 500 W resistive load, and from a 400 W resistive load to an inductive load of 500 W 0.85 power factor lagging. From the simulation results for both cases, the state-of-charge of the battery decreases due to supplying power to the loads, yet the battery voltage remains constant at about 36 V and the battery current exhibits a smooth ripple despite the current spikes produced by the H-bridge inverter, which will prolong the lifespan of the battery. This shows that the DC filter performs satisfactorily to isolate the current spikes generated by the SPWM controller and H-bridge inverter. Moreover, even though the load varies for both cases, the sinusoidal inverter output voltage can be tracked and maintained at 230 V_{rms} with a 50 Hz frequency within a few cycles from the instant that the load is changed, as well as a low total harmonic distortion voltage (THD_v) content of 1.53% and 2.78%, respectively. This indicates that the controller proves its robustness and stiffness characteristics in maintaining the output load voltage at the desired value to supply the power for a variety of loads with a minimum THD_v.

Key words: Stand-alone, single-phase inverter, deadbeat, battery cell, low-pass filter, sinusoidal pulse-width-modulation, PI controller, Butterworth filter

1. Introduction

In the last few decades, the traditional power generation methods of burning fossil fuels has affected the environment, causing an increase in the greenhouse gas emissions that lead to global warming. Consequently, this has become the driving force for the growing interest in alternative energy [1,2]. In order to reduce environmental pollution, sustainable energy electricity generation systems are gaining popularity, and the development of distributed generation (DG) power systems, as well as stationary power generation stand-alone application systems, has become more significant [3,4]. DG power systems can be operated as uninterrupted power systems and dynamic voltage restorers, which maintain high-quality electrical power to critical load installations in the event of voltage sags due to system faults [4]. These systems usually consist of inverters that interface with the loads or sources.

*Correspondence: tl.tiang.ee@gmail.com

However, a battery inverter system is more preferable and more flexible to operate in stand-alone mode applications. The single-phase inverters in stationary battery cell power generation systems have been installed worldwide in case of utility power failures and are widely used in delivering backup power to critical loads, such as for computers and life-support systems in hospitals, hotels, office buildings, schools, utility power plants, and even in airport terminals, as well as in communication systems [5]. In industry, the total harmonic distortion voltage (THD_v) should not exceed 5%, as per the guidelines given in IEEE Standard 519-1992. The inverter must be efficient and comply with the requirements of the harmonic control, interconnection, and safety standards, according to IEEE 1547.

In general, there are many methods for producing a low-distortion output voltage. One of these methods is the optimum fixed LC compensator, which is designed to minimize the expected value of the total THD_v, while it is desirable to maintain a specific value of the power factor (PF) [6,7]. Alternatively, series and shunt compensation or hybrid series active power filters can be employed for the elimination of harmonics when nonlinear loads are connected to an inverter [8,9]. However, the appropriate use of reactive shunt compensators and filters may increase the harmonic current content, as well as the voltage distortion in the feeders of the systems [10]. Moreover, the use of pure capacitive compensators combined with source harmonics would degrade the PF and overload the equipment. In [11], it was shown that series active filters in 2-level pulse-width modulation (PWM)-based inverters have the disadvantages of high-order harmonic noise and additional switching losses due to high-frequency commutation.

In previous research work, there are many control techniques for producing pure sinusoidal output voltages with low THD_v and fast dynamic responses. First, the conventional proportional-integral (PI) or PI-derivative (PID) controllers for the single-phase inverter were presented in [12]. In addition, a proportional-resonance (PR) controller was employed in grid-connected converter systems in [13,14]. Many discrete-time methods developed by low-cost microcontrollers have been designed, such as repetitive-based control [15], sliding mode control [16], and deadbeat-based control [17,18], to enhance the characteristics of the inverter systems. Additionally, a variety control approaches for inverter systems have been reported, including, for instance, neural network-based control [19], fuzzy logic-based control [20], composite observer control [21], internal-model control (IMC) [22], and multiple feedback loop control [23]. The dynamic performance of repetitive control methods is low and requires the accurate values of the filter components, as well as the system stability staying within a narrow operating range. The odd harmonic repetitive control scheme also has a drawback, in that the even harmonic residues occur in the tracking error. In addition, the sliding mode control has been proven to cope with uncertainty, but a chattering problem will occur during hardware implementation. In addition, the IMC-PID controls and multiple feedback loop controls require the sophisticated frequency response analysis of open and closed loops.

Furthermore, several complex control approaches that are difficult to implement have been presented, such as using composite observer control, resonant and PR controllers, neural network-based control, or a phase-shifted PWM algorithm. Additionally, selective harmonic eliminated PWM control and fuzzy logic control in inverter systems were discussed in [24], which are highly dependent on the availability of the memory space of a microcontroller during implementation. In fact, deadbeat control is one of the most attractive techniques for discrete-time control since it is able to reduce the state variable errors to zero in a finite number of sampling steps and provides the fastest dynamic response for digital implementation.

In previous research work, most of the inverters are used in DG power systems for grid-connected applications, but the investigation of stand-alone applications is lacking. In this paper, a stand-alone voltage

source inverter system using a battery cell as the primary energy source is proposed using a deadbeat-based PI controller to produce a quality sinusoidal output voltage. This proposed inverter system illustrates a simple structure with only an output voltage sensor on the load side and demonstrates excellent performance. The proposed single-phase inverter is suitable for residential power generation, especially for stand-alone applications. The control technique also has strong robustness and excellent dynamic and static characteristics. In order to prolong the lifespan of the battery, a capacitor-inductor capacitor (CLC) DC filter should be used to mitigate the ripple currents in stand-alone power generation systems, instead of using the DC active filter.

2. Stand-alone single-phase inverter system

2.1. System configuration

In this paper, a low-voltage harmonic single-phase voltage source inverter system using a lead acid battery as the primary energy source and being controlled by a deadbeat-based PI controller is proposed. Figure 1 shows the schematic circuit and the block diagram of the stand-alone single-phase inverter system, which includes a lead acid battery that is the primary energy source, third-order Butterworth low-pass DC filter, H-bridge inverter power metal oxide semiconductor field-effect transistor (MOSFET), step-up transformer, third-order Butterworth low-pass AC filter, and loads. This inverter system will be simulated in MATLAB/Simulink, and most of the components used can be found in the MATLAB/SimPowerSystems simulation software.

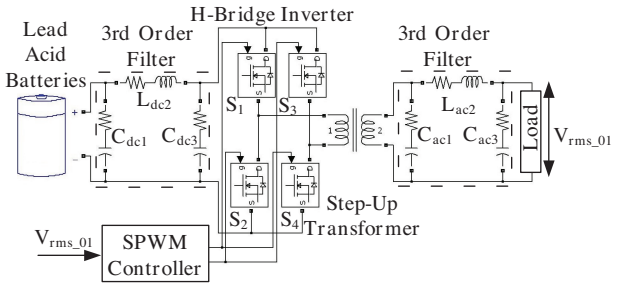

Figure 1. Schematic circuit and block diagram of the stand-alone single-phase inverter system.

In general, the power delivered from the lead acid battery to the loads passes through a few stages. First, the battery injects the power into the CLC DC filter instead of the H-bridge inverter in order to isolate the high peak ripple current created by the switching of the inverter. Next, the DC input voltage is converted to an AC output voltage using a sinusoidal PWM (SPWM) switching scheme for the H-bridge inverter, and the output voltage is then boosted up via a step-up transformer with a transformer ratio of 1:9.6. The secondary AC voltage contains many harmonics due to the switching frequency of the inverter and should be filtered out using a CLC AC low-pass filter to produce a 230 V_{rms} pure sinusoidal output voltage for loads in the stand-alone application system. The magnitude and the frequency of the output voltage are controlled by the deadbeat-based PI SPWM controller, with the feedback signal of the fundamental root mean square (RMS) value of the output voltage.

2.2. Third-order Butterworth low-pass DC filter model

Essentially, the input current ripples will shorten the lifespan of the electrolytic capacitors, batteries, and fuel cells that act as primary energy sources. Therefore, the lead acid battery needs to be connected to a third-order Butterworth low-pass DC filter in order to protect the battery from damage. The DC filter components

constitute 2 capacitors and an inductor. These components have a transfer function that can be realized using a Cauer 1-form. The kth elements of the filter components can be expressed as:

$$C_k^{'} = 2\sin\left(\frac{2k-1}{2n}\pi\right),\ k = \ odd, \tag{1}$$

$$L_k^{'} = 2\sin\left(\frac{2k-1}{2n}\pi\right),\ k = even, \tag{2}$$

where n is the number of passive components, $C_k^{'}$ is the kth capacitance value of the prototype, and k is an odd number. Meanwhile, $L_k^{'}$ is the kth inductance value for the prototype and k is an even number [25]. Next, the DC capacitance and inductance values, C_{dc1}, L_{dc2}, and C_{dc3}, as indicated in Figure 1, can be calculated with the aid of a frequency and impedance scaling technique, as expressed below:

$$Z = \frac{V^2}{P}, \tag{3}$$

$$C_k = \frac{1}{Z\omega_c}C_k^{'}, \tag{4}$$

$$L_k = \frac{Z}{\omega_c}L_k^{'}, \tag{5}$$

where Z is the terminating impedance in Ω, ω_c is the cut-off radian frequency with $\omega_c = 2\pi f_c$, and f_c is the cut-off frequency (100 Hz) [26]. In the simulation model, the capacitance and inductance values for the DC filter for C_{dc1} and C_{dc3} are 872 μF and L_{dc2} is 5.8 mH.

2.3. Single-phase inverter model

In [27], an overview of single-phase inverter topologies developed for small distributed power generators was discussed. There are many types of inverter topologies. However, the traditional buck inverter with a line frequency transformer exhibits robust performance and greater reliability in a circuit, as shown in [27], and is in total agreement with [28], as depicted in Figure 1. It indicates a simple H-bridge voltage source inverter that can be used for conversion from DC to AC voltage, supplying the power to the loads. It is used to produce and regulate the sinusoidal output voltage at 230 V_{rms}, with 50 Hz frequency to various types of loads in stand-alone power generation systems. The output voltage and output current depend on the method of the switching scheme.

2.4. Step-up transformer model

As shown in Figure 1, a linear 2-winding step-up transformer is connected after the H-bridge inverter to increase the primary voltage in order to maintain the output voltage at 230 V_{rms}. The transformer turn ratio in this simulation is 1:9.6 using the following expression:

$$\frac{V_s}{V_p} = \frac{N_s}{N_p}, \tag{6}$$

where V_s is the voltage in the secondary winding, V_p is the voltage in the primary winding, N_s is the number of turns in the secondary winding, and N_p is the number of turns in the primary winding. This approach of using a transformer is preferable because it can act as an isolation transformer to protect the inverter system from the surge and to reduce harmonics [29].

2.5. Third-order Butterworth low-pass AC filter

After boosting the primary voltage using a step-up transformer, the secondary output voltage consists of many distortions as well as harmonics. Therefore, a third-order Butterworth low-pass CLC AC filter should be connected before sending power to the loads, so as to filter out the unwanted harmonics. The calculations for C_{ac1}, L_{ac2}, and C_{ac3}, as indicated in Figure 1, are based on Eqs. (1) to (5). In the simulation, the capacitance and inductance values for the AC filter that have been used for C_{ac1} and C_{ac3} are 31 μF and L_{ac2} is 0.339 H.

The total harmonic distortion of the output voltage can be estimated using:

$$THD_v = \frac{1}{V_{o1}} \left(\sum_{n=2,3,\ldots}^{\infty} V_{on}^2 \right)^{1/2}, \tag{7}$$

where V_{o1} is the RMS value of the fundamental voltage component and V_{on} is the RMS value of the nth harmonic voltage component [30].

3. Proposed deadbeat-based PI controller with the SPWM switching control scheme

In order to maintain and regulate the output voltage at 230 V_{rms} for different types of loads with a 50 Hz constant frequency, a deadbeat-based PI controller with a SPWM switching control scheme is proposed and employed in the single-phase inverter in the stand-alone power generation system, as shown in Figure 2. Furthermore, the Simulink model developed for this controller is illustrated in Figure 3. Basically, the controller is a 3-level PWM inverter with sinusoidal modulation, in which a control signal at a desired output frequency is compared with multilevel triangular waveforms [31].

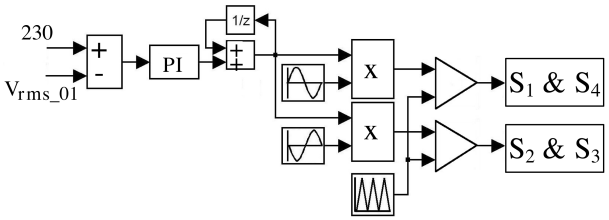

Figure 2. Block diagram of the deadbeat-based PI controller with SPWM switching technique.

In the proposed control scheme, the fundamental RMS value of the output voltage at 50 Hz at the terminal load, V_{rms_01}, will be fed back to the controller and compared with the reference signal of 230 V_{rms}. The difference between the 2 signals is then input into a PI controller to obtain the corresponding and appropriate modulation index, in which the K_p value is 0.0021 and the K_i value is 0.01. The coefficient values of K_p and K_i are computed using a heuristic tuning method, i.e. the Ziegler–Nichols method. In general, the deadbeat controller plays the important role of producing the output voltage to the steady state in finite time steps or dead time after the input signal is applied to the system. Hence, the previous modulation index will be sampled after a delay time of 0.04 s in the model and simulation case study. Subsequently, the modulation index generated by the PI controller will summate with the previous modulation index and send this to the reference sine wave generator. Next, the product of the modulation index and the 2 sinusoidal signals, which are 180° out of phase from each other, will be compared with the triangular signal carriers in order to produce the SPWM switching waveforms used to trigger the 4 power MOSFETs, S_1, S_2, S_3, and S_4, of the H-bridge inverter. The sinusoidal signals used as reference waveforms have a constant frequency of 50 Hz, while the triangular signal carrier is at

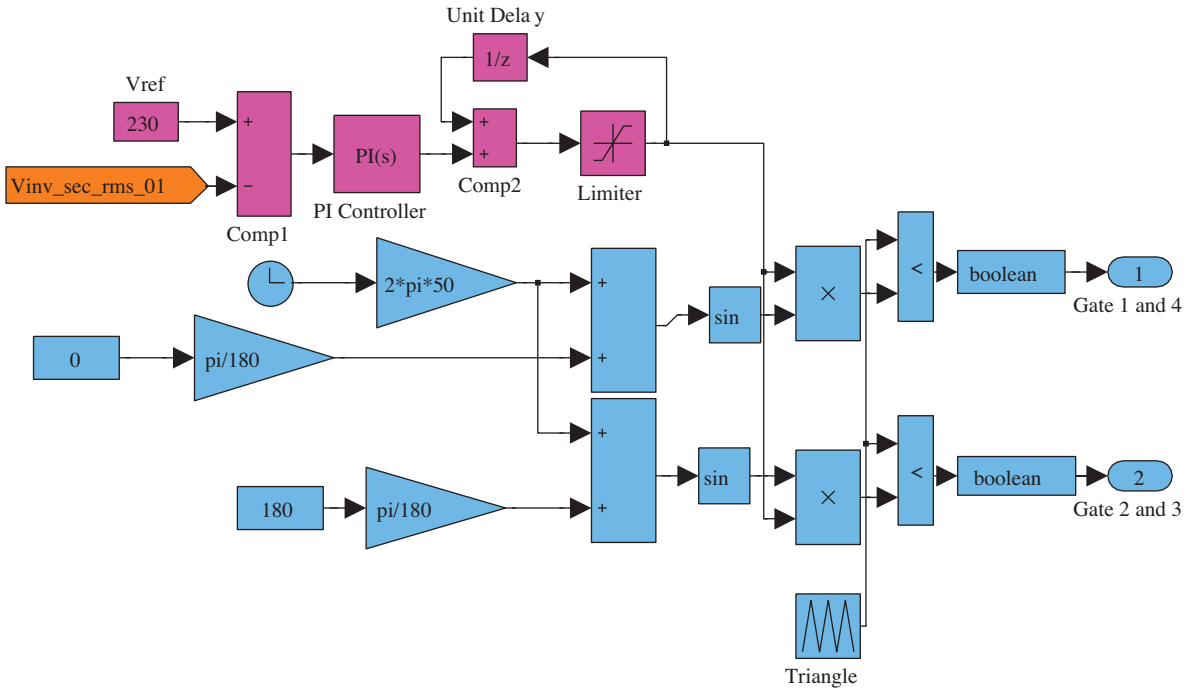

Figure 3. Simulink model of the proposed deadbeat-based PI controller with SPWM switching control scheme.

5 kHz. Therefore, the RMS output voltage can be varied by changing the modulation index, M.

$$M = \frac{A_r}{A_c} \tag{8}$$

Here, A_r is the amplitude of the reference signal and A_c is the amplitude of the control signal. The RMS output voltage, V_{o_rms}, also can be expressed as:

$$V_{o\_rms} = V_s \left(\sum_{m=1}^{2p} \frac{\delta_m}{\pi} \right)^{1/2}, \tag{9}$$

where V_s is the input voltage, δ_m is the width of the mth pulse, and p is the number of pulses per half-cycle. Hence, using this simple controller triggering the MOSFETs as shown in Figure 1, a smooth sinusoidal output voltage of 50 Hz can be regulated and maintained.

4. Simulation results and discussion

The deadbeat-based PI controller is proposed here in order to produce and maintain a constant RMS output voltage of 50 Hz, 230 V_{rms} with negligible harmonic content. A simulation model of the stand-alone single-phase inverter system has been developed, as shown in Figure 4. The Table lists the system configuration and simulation parameters.

Figures 5 and 6 show the SPWM gate signals of S_1 and S_4, as well as the SPWM gate signals for S_2 and S_3 that have been produced by comparing the 50 Hz reference sinusoidal waveforms and the 5 kHz triangular waveform, whereby 1 of the sinusoidal waveforms is 180° out of phase from the other, assuming that

the modulation index is 1.00. In fact, the modulation index of the inverter system keeps changing due to the existence of the deadbeat-based PI controller.

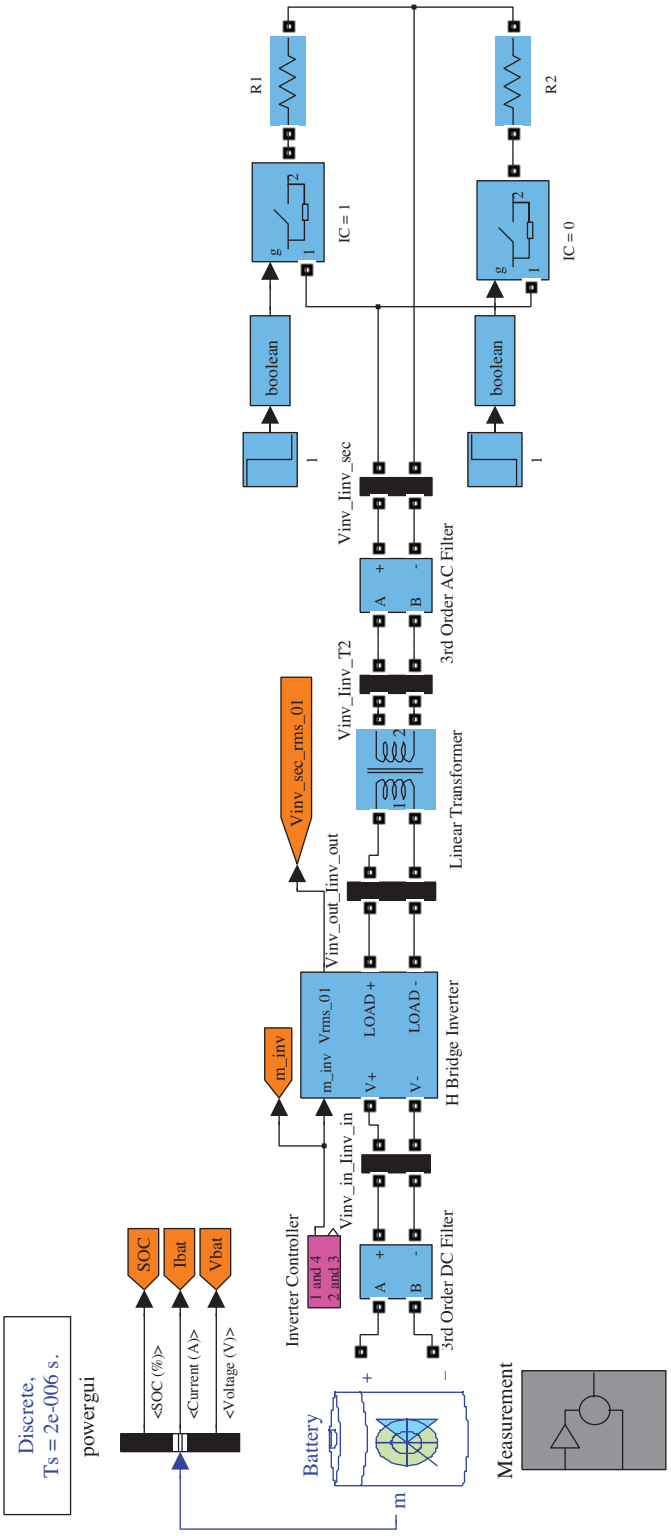

Figure 4. Simulink model of the stand-alone single-phase inverter system.

Table. System configuration and simulation parameters.

Battery supply voltage	36.0 V
Rate capacity	120 Ah
Initial SOC	50 %
$C_{dc1} = C_{dc3}$	872 μF
L_{dc2}	5.8 mH
On resistance, R_{on}	0.0075 Ω
Linear transformer ratio	1:9.6
Line frequency	50 Hz
$C_{ac1} = C_{ac3}$	31 μF
L_{ac2}	0.339 H
Switching frequency	5 kHz
Nominal load voltage	230 V_{rms}
Nominal load frequency	50 Hz
Load R_1	400 W
Load R_2	500 W
Load R_3	500 W, 0.85 PF lagging
K_p	0.0021
K_i	0.01

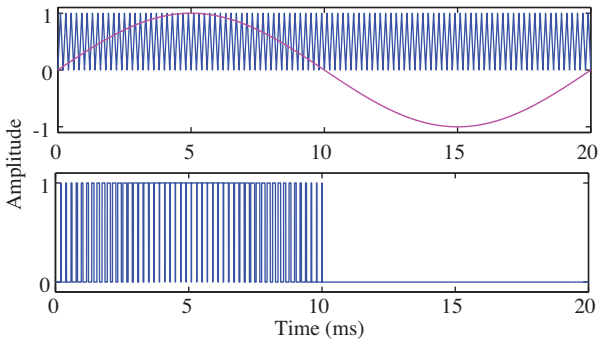

Figure 5. SPWM gate signals S_1 and S_4, produced by comparison of sinusoidal and triangular waveforms.

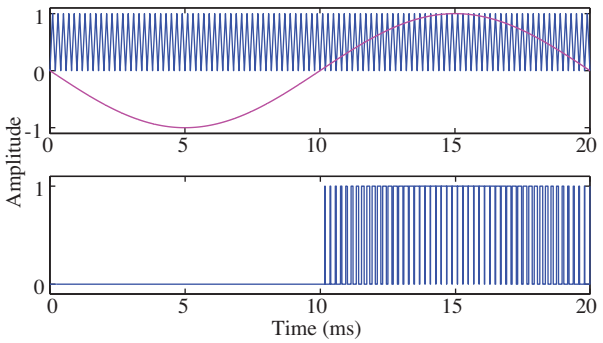

Figure 6. SPWM gate signals S_2 and S_3, produced by comparison of sinusoidal and triangular waveforms.

Figure 7 shows the output voltage and output current when the resistive load is connected to the inverter during the time from 0 s to 1.2 s. The simulation results show that the output voltage and current reach a steady state after 0.5 s onwards. Initially, the resistive load of 400 W is connected to the inverter. This load is then changed to 500 W at 1 s. The performance characteristic of the controller during this load change will be described and discussed further, with several of the simulation results occurring between 0.95 s and 1.2 s.

In the simulation, the performance of the system is tested under 2 types of load change, i.e. a purely resistive load and an inductive load. First, Figures 8–14 show the simulation results for the case where the resistive load changes from 400 W to 500 W. Figures 8–10 show the state of charge (SOC), battery voltage, and battery current, respectively, when the load changes. During the simulation, the SOC of the battery decreases, so the battery is linearly discharging from the start of the simulation. Meanwhile, the battery voltage is almost constant at 35.7 V with significant ripples, and on the other hand, the battery current is in the range of 18 A to 26 A. It shows smooth ripples instead of spiking voltages and currents produced by the H-bridge inverter MOSFETs, as shown in Figures 11 and 12, due to the components of the DC low-pass filter. Moreover, Figure

13 shows the output voltage and output current at the load terminal when the load changes. During the step response of the load changes, the output voltage, which initially stays at 230 V_{rms}, experiences a sudden decrease in magnitude and slowly ramps up to 230 V_{rms} within 4 cycles. Furthermore, Figure 14 shows that a good sinusoidal output voltage can be realized after the sudden change in loads, whereby the THD_v of the last 2 cycles of the inverter output voltage is about 1.53%. This indicates that the AC filter exhibits good performance in filtering out unwanted frequency components. The phase of the output voltage is the same as the phase of the output current since the step change occurs within a purely resistive load. Hence, the deadbeat-based PI controller is operating satisfactorily to maintain the inverter output voltage magnitude at 230 V_{rms} with low-voltage harmonics.

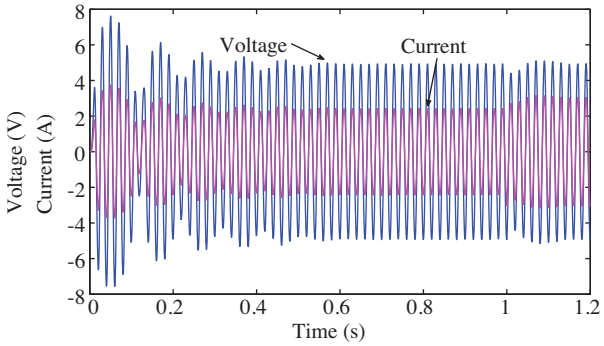

Figure 7. Output voltage and output current when the resistive load changes from 400 W to 500 W at 1 s (voltage: 65 V div^{-1}, current: 1.0 A div^{-1}).

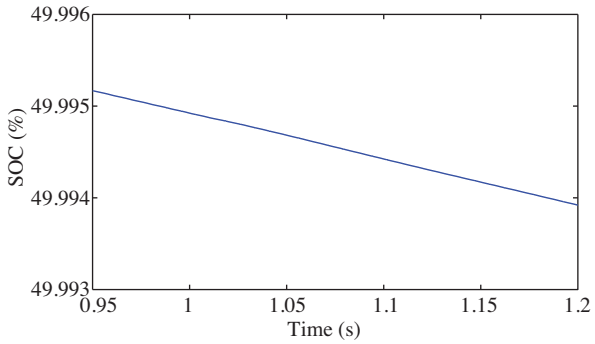

Figure 8. SOC of the battery when the resistive load changes from 400 W to 500 W.

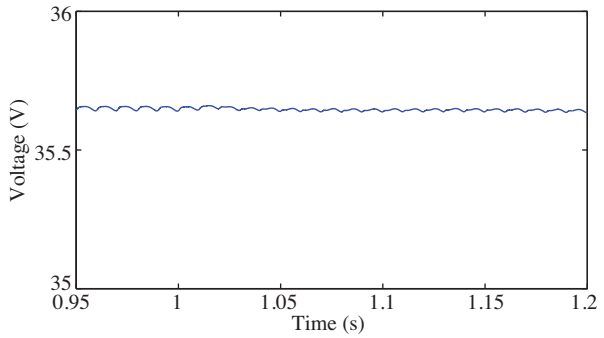

Figure 9. Terminal voltage of the battery when the resistive load changes from 400 W to 500 W.

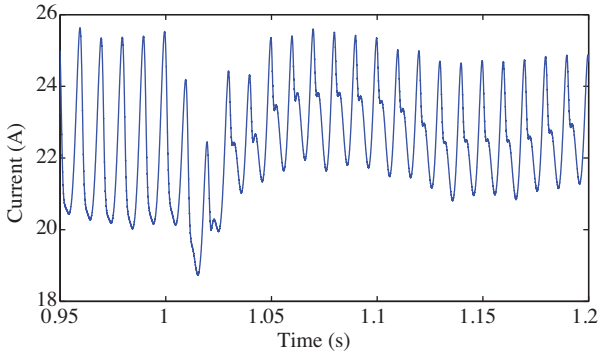

Figure 10. Terminal current of battery when the resistive load changes from 400 W to 500 W.

Secondly, Figures 15–21 present the simulation results for the case where the connected load is changed from a resistive load of 400 W to an inductive load of 500 W with 0.85 PF lagging. Figures 15–17 illustrate the SOC, battery voltage, and battery current during the load change, respectively. It can be clearly seen that the battery is in discharge mode in order to deliver power to the load by observing that the SOC is decreasing linearly, which is almost the same as in Figure 8. In the meantime, the battery voltage is kept constant at about 35.7 V with negligible ripples and is similar to that in Figure 9. Before the step load change takes place, the ripple waveforms are similar to those in Figures 9 and 16; however, after the load changes, in both cases, the ripple waveforms are different due to the connected inductive load. As can be observed, the terminal current of

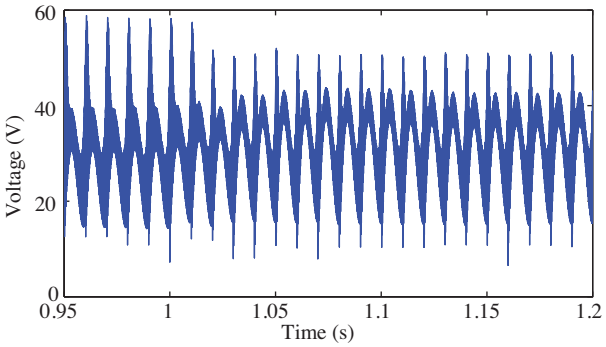

Figure 11. Output voltage after the low-pass DC filter when the resistive load changes from 400 W to 500 W.

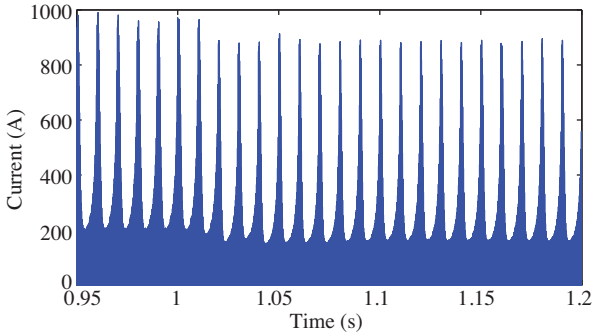

Figure 12. Output current after the low-pass DC filter when the resistive load changes from 400 W to 500 W.

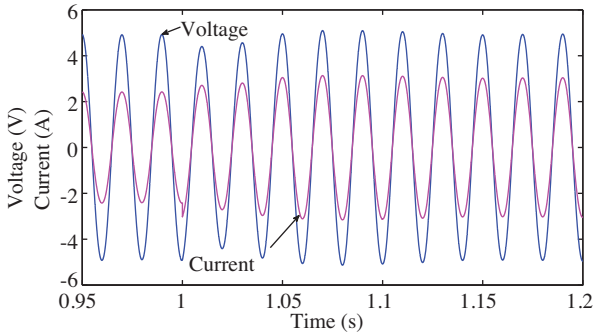

Figure 13. Output voltage and output current when the resistive load changes from 400 W to 500 W (voltage: 65 Vdiv^{-1}, current: 1.0 Adiv^{-1}).

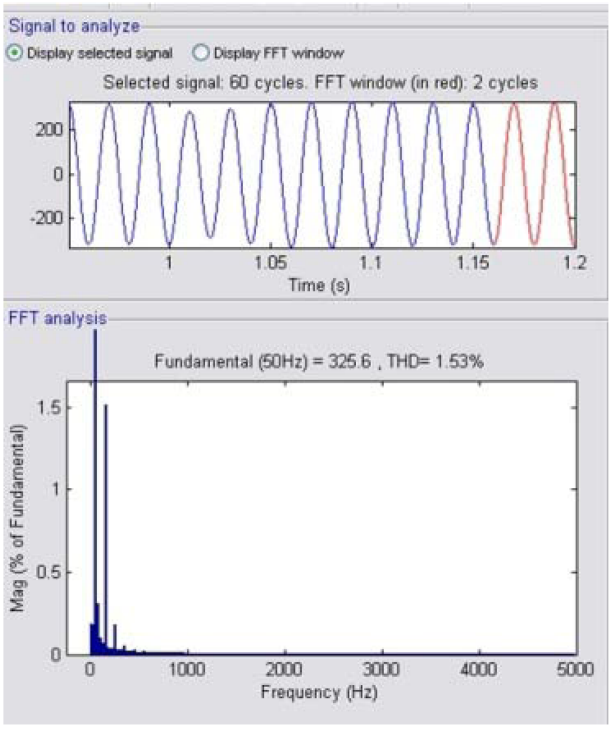

Figure 14. THDv of the output voltage when the resistive load changes from 400 W to 500 W.

the battery exhibits smooth ripples instead of the spiking voltage and current indicated in Figures 18 and 19, which proves the excellent performance of the low-pass DC filter. In addition, the output voltage and output current of the load during the occurrence of the abrupt load changes can be seen in Figure 20. Initially, the output voltage is 230 V_{rms}, and during this transient, the magnitude of the output voltage decreases, but it ramps back up to 230 V_{rms} within 4 cycles. Similarly, the inverter output current shows the same transient pattern as that of the output voltage during this load change. Moreover, the magnitude of the inverter output current is increased due to the higher load and lower PF. Furthermore, a smooth sinusoidal inverter output voltage can be seen, although the inverter system is subjected to sudden load changes. Based on Figure 21, the THD_v of the last 2 cycles of the inverter output voltage is about 2.78%, indicating the high quality of the filter components. With a resistive load, the voltage and current waveforms should be in phase, as shown in Figure 13, whereas the current should be slightly lagging the voltage, as shown in Figure 20, when the load is partially inductive. From these results, the proposed deadbeat-based PI controller shows the evidence of its robust characteristics in maintaining the inverter output voltage magnitude at 230 V_{rms} with low-voltage harmonics, even when the load is inductive at 0.85 PF.

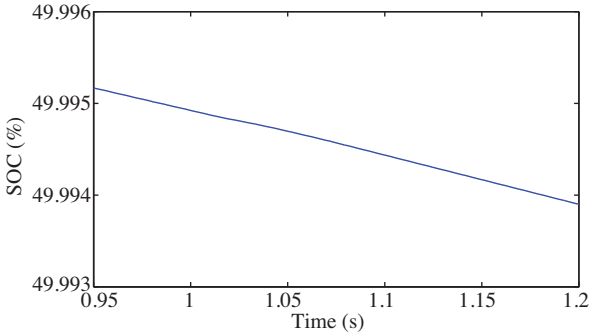

Figure 15. SOC of the battery when the load changes from a resistive load of 400 W to an inductive load of 500 W with 0.85 PF lagging.

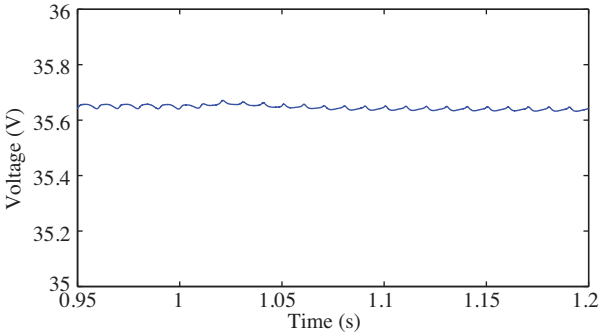

Figure 16. Terminal voltage of the battery when the load changes from a resistive load of 400 W to an inductive load of 500 W with 0.85 PF lagging.

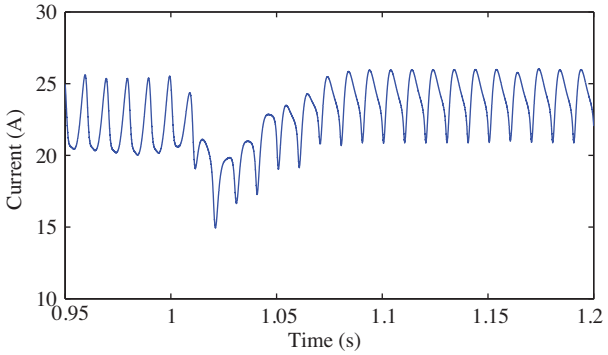

Figure 17. Terminal current of the battery when the load changes from a resistive load of 400 W to an inductive load of 500 W with 0.85 PF lagging.

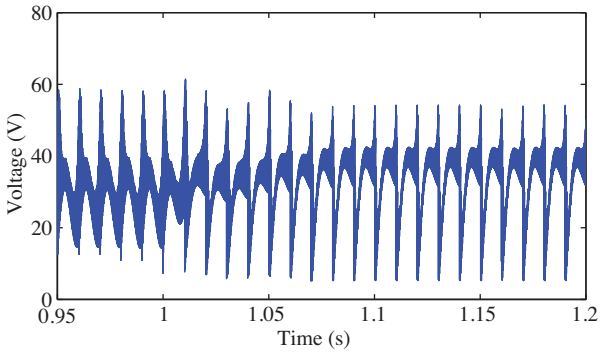

Figure 18. Output voltage after the low-pass DC filter when the load changes from a resistive load of 400 W to an inductive load of 500 W with 0.85 PF lagging.

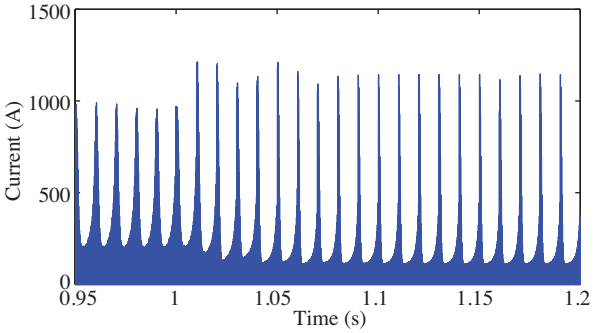

Figure 19. Output current after the low-pass DC filter when the load changes from a resistive load of 400 W to an inductive load of 500 W with 0.85 PF lagging.

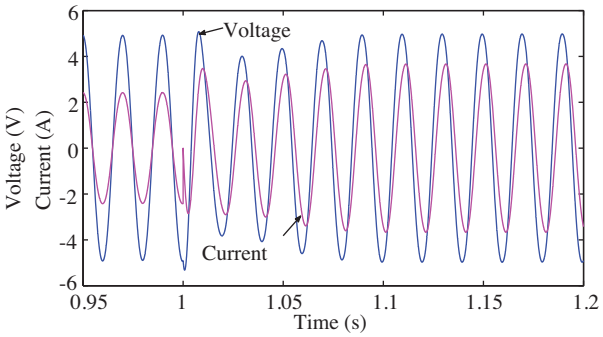

Figure 20. Output voltage and output current when the load changes from a resistive load of 400 W to an inductive load of 500 W with 0.85 PF lagging (voltage: 65 V div^{-1}, current: 1.0 A div^{-1}).

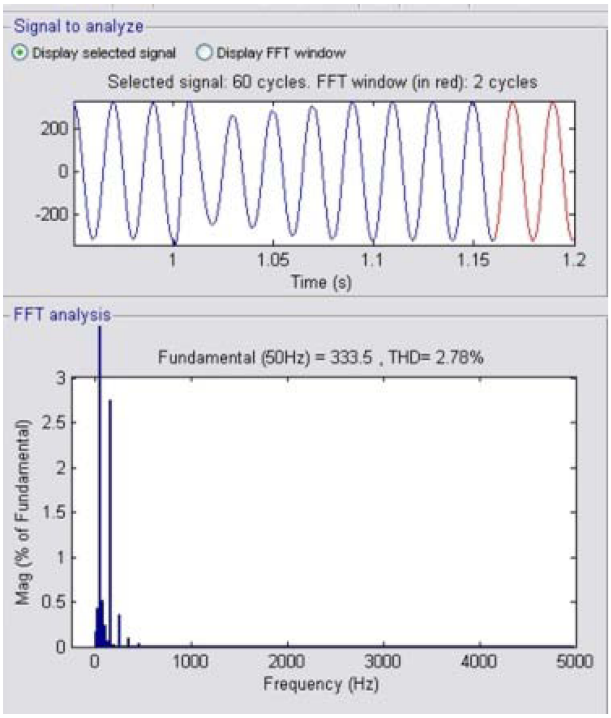

Figure 21. THDv of the output voltage when the load changes from a resistive load of 400 W to an inductive load of 500 W with 0.85 PF lagging.

5. Conclusion

A low-voltage harmonic stand-alone single-phase voltage source inverter using a battery cell as the primary energy source and being controlled by a simple deadbeat-based PI controller has been simulated in MATLAB/Simulink software. The simulation results show that a proper SPWM control switching scheme associated with the deadbeat-based PI controller has been generated to control the H-bridge inverter MOSFETs, where its modulation index can be changed according to the feedback signal of the fundamental output voltage. Moreover, in the simulation of the load changes within a purely resistive load, the battery discharges to supply the

power while the battery voltage is kept constant, and the battery current presents fewer spikes due to the good performance of the DC filter, which will extend the battery's lifespan. The output voltage also shows a good sinusoidal waveform of 230 V_{rms} with only 1.53% THD_v after the load changes, proving that the controller exhibits fast dynamic performance as well as effective filter components. The output currents are in phase with the output voltage due to a purely resistive load. Furthermore, in the case of load changes from a resistive load to an inductive load, the inverter is still able to produce sinusoidal waveforms with 2.78% THD_v, and the voltage is maintained at 230 V_{rms} within a few cycles of being subjected to abrupt load changes. This proves that the deadbeat-based PI controller demonstrates very good performance and possesses robust characteristics in tracking the output voltage at the desired value.

Acknowledgments

The authors of this paper would like to express their appreciation and sincere gratitude to Universiti Sains Malaysia for providing funding for this project through a PRGS grant.

References

[1] J.I. Itoh, F. Hayashi, "Ripple current reduction of a fuel cell for a single-phase isolated converter using a DC active filter with a center tap", IEEE Transactions on Power Electronics, Vol. 25, pp. 550–556, 2010.

[2] S.H. Lee, S.G. Song, S.J. Park, C.J. Moon, M.H. Lee, "Grid-connected photovoltaic system using current-source inverter", Solar Energy, Vol. 82, pp. 411–419, 2008.

[3] M. Delshad, H. Farzanehfard, "A new soft switched push pull current fed converter for fuel cell applications", Energy Conversion and Management, Vol. 52, pp. 917–923, 2010.

[4] H.M. Tao, J.L. Duarte, M.A.M. Hendrix, "Line-interactive UPS using a fuel cell as the primary source", IEEE Transactions on Industrial Electronics, Vol. 55, pp. 3012–3021, 2008.

[5] A. Kawamura, T. Haneyoshi, R.G. Hoft, "Deadbeat controlled PWM inverter with parameter estimation using only voltage sensor", IEEE Transactions on Power Electronics, Vol. 3, pp. 118–125, 1988.

[6] X.Q. Guo, W.Y. Wu, H.R. Gu, "Modeling and simulation of direct output current control for LCL-interfaced grid-connected inverters with parallel passive damping", Simulation Modelling Practice and Theory, Vol. 18, pp. 946–956, 2010.

[7] A.F. Zobaa, "Voltage harmonic reduction for randomly time-varying source characteristics and voltage harmonics", IEEE Transactions on Power Delivery, Vol. 21, pp. 816–822, 2006.

[8] A. Varschavsky, J. Dixon, M. Rotella, L. Moran, "Cascaded nine-level inverter for hybrid-series active power filter, using industrial controller", IEEE Transactions on Industrial Electronics, Vol. 57, pp. 2761–2767, 2010.

[9] F.P. Zeng, G.H. Tan, J.Z. Wang, Y.C. Ji, "Novel single-phase five-level voltage-source inverter for the shunt active power filter", IET Power Electronics, Vol. 3, pp. 480–489, 2010.

[10] J.A. Pomilio, S.M. Deckmann, "Characterization and compensation of harmonics and reactive power of residential and commercial loads", IEEE Transactions on Power Delivery, Vol. 22, pp. 1049–1055, 2007.

[11] J. Dixon, L. Moran, "Multilevel inverter, based on multi-stage connection of three-level converters scaled in power of three", IEEE 28th Annual Conference of the Industrial Electronics Society, pp. 886–891, 2002.

[12] O.Ö. Mengi, İ.H. Altaş, "Fuzzy logic control for a wind/battery renewable energy production system", Turkish Journal of Electrical Engineering & Computer Sciences, Vol. 20, pp. 187–206, 2012.

[13] A. Khairy, M. Ibrahim, N. Abdel-Rahim, H. Elsherif, "Comparing proportional-resonant and fuzzy-logic controllers for current controlled single-phase grid-connected PWM DC/AC inverters", IET Conference on Renewable Power Generation, pp. 1–6, 2011.

[14] G.H. Zeng, T.W. Rasmussen, "Design of current-controller with PR-regulator for LCL-filter based grid-connected converter", 2nd IEEE International Symposium on Power Electronics for Distributed Generation Systems, pp. 490–494, 2010.

[15] K.L. Zhou, K.S. Low, D.W. Wang, F.L. Luo, B. Zhang, Y.G. Wang, "Zero-phase odd-harmonic repetitive controller for a single-phase PWM inverter", IEEE Transactions on Power Electronics, Vol. 21, pp. 193–201, 2006.

[16] W.G. Yan, J.G. Hu, V. Utkin, L.Y. Xu, "Sliding mode pulsewidth modulation", IEEE Transactions on Power Electronics, Vol. 23, pp. 619–626, 2008.

[17] S. Dalapati, C. Chakraborty, "Dynamic performance of a dead-band controlled capacitor charging type inverter", Simulation Modelling Practice and Theory, Vol. 17, pp. 911–934, 2009.

[18] P. Mattavelli, "An improved deadbeat control for UPS using disturbance observers", IEEE Transactions on Industrial Electronics, Vol. 52, pp. 206–212, 2005.

[19] H. Deng, R. Oruganti, D. Srinivasan, "A neural network-based adaptive controller of single-phase inverters for critical applications", 5th International Conference on Power Electronics and Drive Systems, pp. 915–920, 2003.

[20] A. Sakhare, A. Davari, A. Feliachi, "Fuzzy logic control of fuel cell for stand-alone and grid connection", Journal of Power Sources, Vol. 135, pp. 165–176, 2004.

[21] K. Selvajyothi, P.A. Janakiraman, "Reduction of voltage harmonics in single phase inverters using composite observers", IEEE Transactions on Power Delivery, Vol. 25, pp. 1045–1057, 2010.

[22] Y.N. Xu, Y. Zhao, Y. Kang, R. Xiong, "Study on IMC-PID control for single-phase voltage-source UPS inverters", 3rd IEEE Conference on Industrial Electronics and Applications, pp. 824–828, 2008.

[23] N.M. Abdel-Rahim, J.E. Quaicoe, "Analysis and design of a multiple feedback loop control strategy for single-phase voltage-source UPS inverters", IEEE Transactions on Power Electronics, Vol. 11, pp. 532–541, 1996.

[24] R. Akkaya, A.A. Kulaksiz, "A microcontroller-based stand-alone photovoltaic power system for residential appliances", Applied Energy, Vol. 78, pp. 419–431, 2004.

[25] A. Timar, M. Rencz, "Design issues of a low frequency low-pass filter for medical applications using CMOS technology", Proceedings of the IEEE Workshop on Design and Diagnostics of Electronic Circuits and Systems, pp. 325–328, 2007.

[26] M. Kaufman, J.A.S. Wilson, P. Brooks, Schaum's Outline of Theory and Problems of Electronics Technology, New York, McGraw-Hill, 1982.

[27] Y.S. Xue, L.C. Chang, K. Sren Baekhj, J. Bordonau, T. Shimizu, "Topologies of single-phase inverters for small distributed power generators: an overview", IEEE Transactions on Power Electronics, Vol. 19, pp. 1305–1314, 2004.

[28] S.M. Jung, Y.S. Bae, S.W. Choi, H.S. Kim, "A low cost utility interactive inverter for residential fuel cell generation", IEEE Transactions on Power Electronics, Vol. 22, pp. 2293–2298, 2007.

[29] N. Mohan, T.M. Undeland, W.P. Robbins, Power Electronics: Converters, Applications, and Design, 3rd ed., New York, Wiley, 2003.

[30] M.H. Rashid, Power Electronics, Circuits, Devices and Applications, 3rd ed., Pearson Education, Upper Saddle River, NJ, USA, Prentice Hall, 2004.

[31] A.W. Leedy, R.M. Nelms, "A general method used to conduct a harmonic analysis on carrier-based pulse width modulation inverters", Simulation, Vol. 87, pp. 205–220, 2010.